REVIEWED

Surface tension of fuels – Analysis of measurement methods and applicability on rail-pressure environments

Marcel Rückert*, Olivier Reinertz* and Katharina Schmitz*

RWTH Aachen University, Institute for Fluid Power Drives and Systems (IFAS), Campus-Boulevard 30, D-52074 Aachen, Germany*
E-Mail: Marcel.Rueckert@ifas.rwth-aachen.de

Spray characteristics during the injection process of a combustion system, bubble formation in chemical reactors or hydraulic fluids all share surface tension as a key variable regarding aforementioned behaviours. Depending on the system liquid-liquid or liquid-gas interphases play a defining role. In this work, the most relevant measurement methods are discussed. Based on the Du Noüy method, the surface tension of common fuels and mixtures is measured and presented. The measurements do illustrate the influence of mixture components on surface tension as the behaviour can be strongly non-linear. Additionally, the applicability of the aforementioned measurement methods on high-pressure environments is investigated and a possible solution for measurements up to multiple 100 MPa is introduced. With liquid-air interphases being quite difficult to handle at high pressures, an assessment is made for nitrogen regarding it´s properties und extreme conditions.

Keywords: Surface tension, Fuel, High-pressure, Fluid properties
Target audience: Tribology & Fluids, Design Process

1 Introduction

Within the cluster of excellence "Tailor-Made Fuels from Biomass" at RWTH Aachen University, a team of researchers is investigating new biofuel candidates from production to propulsion. The main foci of research are the chemical reaction paths for an industrial scale production, fluid analytics and simulation as well as necessary adaptions and improvements of the combustion system.

Amongst others, a suitable biofuel candidate combines advantageous rheological properties regarding the combustion process many of which are in direct opposition to each other. Volumetric losses in common-rail injection pumps, which are lubricated by the fuel itself, can be reduced by using a fuel with elevated viscosity. Looking at the injector, a higher viscosity leads to a limited performance, effectively reducing the overall combustion efficiency and increasing soot emissions. The reason for this phenomenon is the increased friction of the fluid, causing reduced mass flow. Another vital factor for fluid properties regarding injector performance is the spray distribution behaviour. One way to characterise spray is the dimensionless Ohnesorge number *Oh*, see equation (1) /1/. Here, the internal viscosity dissipation is related to the surface tension energy. For lower Ohnesorge numbers, the friction losses due to viscous forces are weak and the energy converts into surface tension energy enabling the formation of droplets /2/. Figure 1 shows the Ohnesorge number plotted over the Reynolds number *Re* to distinguish different spray areas: Rayleigh breakup, windinduced breakup, which accounts for two different areas depending on jet velocity and oscillation, and atomisation /3/. In order to ensure a homogeneous spray distribution in the combustion chamber, injectors work with Ohnesorge numbers far below 0.1, see Figure 1.

$$Oh = \frac{\eta}{\sqrt{L \cdot \sigma \cdot \rho}} \tag{1}$$

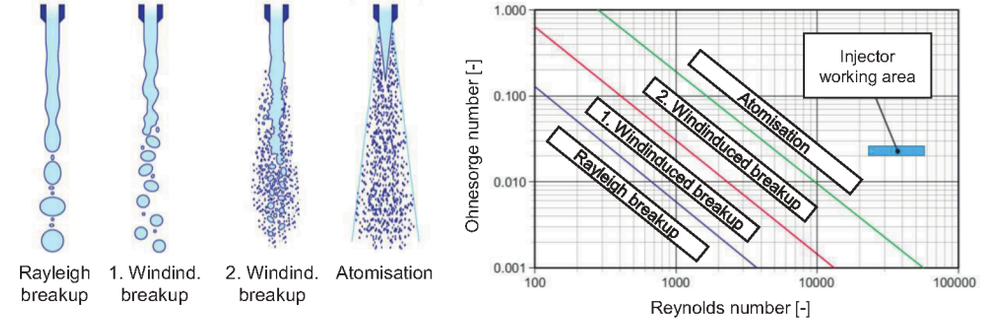

Figure 1: Different spray areas depending on Ohnesorge- and Reynolds number after /3/.

In order to design new injection systems or tune existing technology to perform in an optimal way using innovative biofuel candidates, fluid characteristics need to be known. Especially surface tension is a key property not only for the design of injectors, but also for chemical reactors, see /4/.

Looking at hydraulics, cavitation as a whole has been a defining and relevant topic. Damages or reduced performance due to cavitation are subject to current research, see /5/ and /6/. The ascension speed of a bubble inside hydraulic oil can be described with Equation (3) using the Young-Laplace Equation (2) to substitute the bubble radius with the surface tension, see /7/. Here, the speed has a quadratic dependency on surface or interface tension between bubble and oil. This phenomenon is highly relevant for design and simulation of hydraulic reservoirs, where air bubbles need to leave the oil as fast as possible. Additionally, latest and more sophisticated modelling of cavitation requires surface tension as an input parameter. In order to increase simulation accuracy, this parameter needs to be known over a wide range of pressure and temperature.

$$\left(p_{bubble} - p_{fl}\right) = \frac{2 \cdot \sigma}{r} \tag{2}$$

$$v = \frac{2}{9}\left(\rho_{fl} - \rho_{bubble}\right)\frac{r^2 g}{\eta} = \frac{8}{9} \cdot \frac{\left(\rho_{fl} - \rho_{bubble}\right) \cdot g \cdot \sigma^2}{\eta \cdot \left(p_{bubble} - p_{fl}\right)^2} \tag{3}$$

Looking at binary mixtures, surface tension can be highly non-linear, see Figure 2. Here, a mixture of water and different weight fractions w_2 of sulfuric acid and Diethylene-glycol-diethyl-ether (dgde) respectively was investigated at 293 K and ambient pressure /8, 9/. Since the mixture-behaviour strongly differs depending on the partners, analytical modelling is only possible to a certain extent. Therefore, empirical data is needed to provide accurate input for simulation and design purposes.

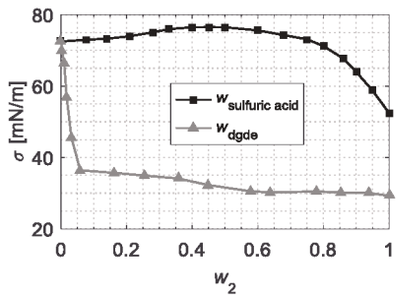

Figure 2: Surface tension of water-sulfuric acid and water-dgde mixture over the mass fraction after /8, 9/.

1.1 Pressure dependency

For combustion systems, chemical reactors and fluid power systems in general, the assumption that the effects of surface tension only play a role at ambient pressure is hardly true. Depending on the operational strategy of an engine and the pressure level of chemical reactors and fluid power systems, surface tension is relevant at a wide range of pressures and temperatures. The pressure dependency of surface tension can be seen in Figure 3. Here, diesel was measured with a gaseous nitrogen atmosphere at pressure levels up to 9.4 MPa using the capillary wave method, see /10/. The change in surface tension at 9.4 MPa compared to ambient pressure can be computed to 28%. For natural water in a methane atmosphere, see /11/, the change of surface tension at 21 MPa compared to ambient conditions is 21%. For measurements up to 40 MPa, the pendant drop method was used. The measurements were done at 298 K. Both values indicate a highly pressure-dependent behaviour of surface tension. In order to do high-pressure measurements, a suitable technique has to be identified. In the following, prominent methods for measuring surface tension are introduced and advantages as well as disadvantages of each method are discussed.

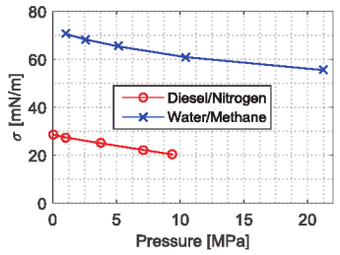

Figure 3: Pressure-dependency of surface tension for water in a methane atmosphere and diesel in an nitrogen atmosphere after /10, 11/.

2 Measurement methods

The determination of surface tension can be done using different methods. In the following, the most relevant methods will be introduced and an evaluation regarding the applicability in high-pressure measurements is done. First of all, the measurement principles are categorised in four groups: Resistance, droplet, capillary and frequency based methods.

2.1 Resistance based measurements

The measurement of surface tension can be done by dragging a body through the surface of the fluid in question. Figure 4 shows the different principles of measurement: Wilhelmy plate method, Du Noüy ring method and wire method.

The Wilhelmy method uses a thin plate mostly made of roughened platinum-iridium alloy or platinum which is cleaned and flamed before every measurement. Then, the plate is put in a fixed position relative to the horizontal liquid surface. A vertical force F is applied to the plate while it is being lifted from the liquid. Due to surface tension, a liquid meniscus originates. The weight of the meniscus equals the pulling force in equilibrium. With knowledge of force F, thickness t and length L of the plate as well as the meniscus angle φ, the surface tension can be calculated using equation (4) /12/.

$$\sigma = \frac{F}{2(L+t)\cdot\cos\varphi} \tag{4}$$

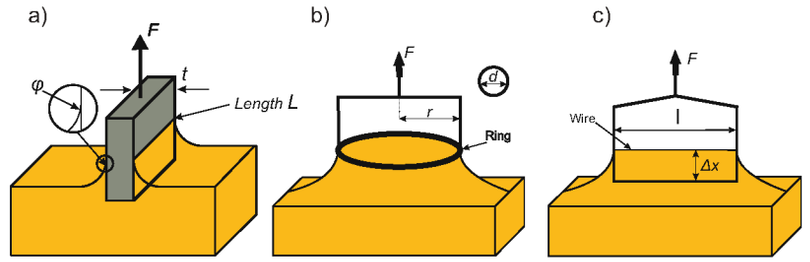

Figure 4: Surface tension measurement methods: Wilhelmy method a), Du Noüy method b), wire method c).

Using the Du Noüy method, the force F is measured which is required to pull a ring made of platinum-iridium alloy or platinum out of a liquid surface. The ring has a wire diameter d and a radius r. Pulling the ring through the liquid surface, a meniscus rises with the ring. Using a microscale, force F equals the weight of the liquid meniscus. Surface tension can be calculated at the point where the meniscus collapses, using equation (5). At the point of a collapsing meniscus, the angle φ is approximately zero which results in $cos\ \varphi$ being unity. Additionally, a correction factor f is needed, which can be calculated after the measurement, see equation (6). For measurement purposes, smaller rings are favoured due to bigger correction factors /12/. The wire method works with the same principle than the Du Noüy method. Instead of a ring, a straight, thin wire is used. The forces measured therefore are smaller and finer microscales are needed.

$$\sigma = \frac{F}{4\pi r\cdot\cos\varphi}\cdot f \approx \frac{F}{4\pi r}\cdot f \tag{5}$$

$$f = 0.725 + \left(\frac{9.075\cdot 10^{-4}F}{\pi^3\Delta\rho g r^3} - \frac{1.679d}{2r} + 0.04534\right) \tag{6}$$

In general, all the above mentioned methods are applicable in high-pressure surroundings, since the measurements do not take up much space and can be integrated into pressure chambers. Additionally, the force measurements do not rely on optical evaluation and can be completely immersed in the test fluid. For the Wilhelmy method, a sensor to evaluate the angle between meniscus and plate needs to be incorporated in the pressure chamber as well. Here, pressure limits are set due to the optical nature of this measurement. Additionally, not all liquids can be measured with the Wilhelmy method, since the surface energy of the plate can be influenced by non-ionic surfactants for example. The Du Noüy method on the other hand only needs a force measurement due to the meniscus angle being approximately zero. Compared to the wire method, the force sensor has to detect approximately three times higher forces. With forces being in the order of mN, higher forces equal higher accuracy. When done correctly, the Du Noüy method provides the highest accuracy out of the aforementioned methods /12/.

2.2 Droplet-based measurements

Droplet based measurements can range from simply to set up methods to highly complex test rigs. Figure 5 shows the three primary methods: Pendant drop method, spinning drop method and drop volume method.

For the pendant drop method, the equatorial diameter d_e and the additional diameter d_s at the drop height d_e need to be measured, see Figure 5 *a)*. Calculation of the surface tension can be done using equation (7). Here, the shape dependent parameter H needs to be calculated using empirical data /13/. The pendant drop method requires high cleanliness and a capillary which is adjusted to the drop geometry. The recommended capillary diameter is less than 0.5 d_e but should not be too small, since d_s is directly influenced by the capillary diameter.

$$\sigma = \frac{\Delta\rho g d_e^2}{H} \tag{7}$$

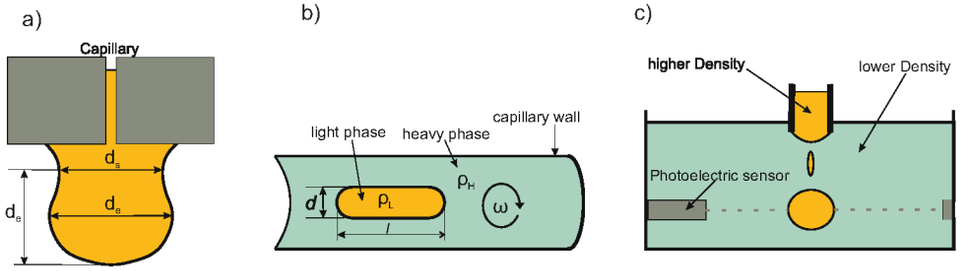

Figure 5: Surface tension measurement methods: Pendant drop method a), spinning drop method b), drop volume method c).

The spinning drop method, as presented in Figure 5 *b)*, is a method to study ultralow surface tension values down to 10^{-6} mN/m /14/. In a horizontal tube, a droplet of lower density than the surrounding fluid is spun with rotational velocity ω. At sufficiently high speeds, the droplet becomes cylindrical. The resulting diameter d is a result of the surface tension, which can be calculated using equation (8).

$$\sigma = \frac{1}{32} d^3 \Delta\rho \omega^2 \tag{8}$$

For the drop volume method, seen in Figure 5 *c)*, the volume V of a drop falling from a capillary with a radius r is determined by using a photoelectric sensor for example. With the drop volume and the capillary radius, the surface tension can be calculated using equation (9) with f being a correction factor as a function of $r/V^{1/3}$, see equation (10) /15/. A weak point of this method is the vulnerability to minor vibrations. These can cause the premature ejection of droplets before reaching the critical mass resulting in inaccurate measurements.

$$\sigma = \frac{V \Delta\rho g}{2\pi r^2 f\left(\frac{r}{\sqrt[3]{V}}\right)} \tag{9}$$

$$f\left(\frac{r}{\sqrt[3]{V}}\right) = 0.167 + 0.193\left(\frac{r}{\sqrt[3]{V}}\right) - 0.0489\left(\frac{r}{\sqrt[3]{V}}\right)^2 - 0.0496\left(\frac{r}{\sqrt[3]{V}}\right)^3 \tag{10}$$

The applicability of droplet-based measurements to high-pressure surroundings highly depends on the method in question. The spinning-drop-method for example requires a transparent tube to evaluate the drop geometry. Using specific material, a transparent pressure tube could be manufactured. Nevertheless, this cannot compensate the drawback only liquid-liquid measurements can be conducted with this method. The drop volume method requires high precision sensors to determine the volume of the droplets. With such a precision sensor integrated into high-pressure, only certain pressure-levels can be reached without damaging the sensor itself or influencing the principle on which the sensor is based. Measurements at elevated pressures based on the pendant-drop-method have been conducted already, see /11/. Here the pressure range is also limited due to the optical nature of the method. Additionally, depending on viscosity and surface tension, a change of capillaries at higher pressure levels might be necessary. This means, that the equilibrium is disturbed and measurement in itself can be questioned.

2.3 Capillary-based measurements

The surface inside a capillary can also be used to evaluate surface tension. Figure 6 shows two options: Capillary rise method and capillary flow method.

With the capillary rise method the height h of a meniscus in a round glass tube with inner diameter d is measured. If the tube diameter is small compared to the tube height, the meniscus has an almost spherical shape, making the cosine of the contact angle between meniscus and tube unity. In case of a spherical meniscus, equation (11) can be applied. For non-spherical menisci, equation (12) applies /12/. The challenge using the capillary rise method is the uniformity of the inner diameter of the glass tube. Additionally, this method is not suitable for liquid-liquid interfaces.

$$\sigma = \frac{\Delta\rho g h d}{4\cos\varphi} \tag{11}$$

$$\sigma = \frac{1}{2}\Delta\rho g r h \cdot \left(1 + \frac{r}{3h} - 0.1288\frac{r^2}{h^2} + 0.1312\frac{r^3}{h^3}\right) \tag{12}$$

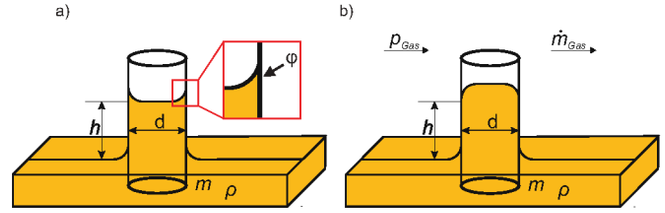

Figure 6: Surface tension measurement methods: Capillary rise method a), capillary flow method b).

Based on the same principle, the capillary flow method, see Figure 6 b), uses a gas which flows over a glass tube. Inside the tube, the geometry of the meniscus can be evaluated and the surface tension calculated. The same problems regarding manufacturing apply to this method as well, which means that liquid-liquid measurements are challenging to realise.

Both of the above mentioned methods do show significant problems regarding high-pressure applicability. With glass being highly brittle, hydrostatic loads can cause cracking of the glass tube. The manufacturing challenges regarding a uniform glass tube also add to this list. Additionally, the capillary flow method requires a fluid flow over the capillary. At high pressures, this flow is difficult to realise. Without possibility of measuring liquid-liquid surfaces, these methods are not suited for the aspired high-pressure measurements.

2.4 Frequency-based measurements

In order to measure the dynamic surface tension, two different approaches can be made: Oscillating drop method and the capillary wave method, shown in Figure 7.

The oscillating drop method evaluates the surface tension of an expanding and collapsing droplet hanging from a capillary. Using a pump, the pressure of the droplet can be varied and different pressure drops can be evaluated while continuously monitoring geometry and pressure of the droplet. The capillary wave method on the other hand uses a needle to create waves on the surface of a liquid. The wave frequency and length can be measured to calculate the surface tension. This method was already used for measurements of different fuel candidates at pressures up to 9.4 MPa, see /11/.

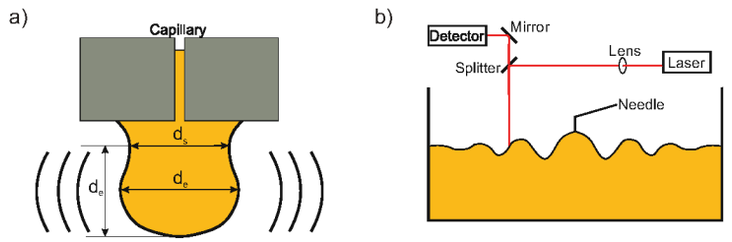

Figure 7: Surface tension measurement methods: Oscillating drop method a), capillary wave method b).

Nevertheless, usability of these methods for high-pressure measurements is limited due to the required optical measurement devices. Additionally, this method is difficult to realise with a liquid-liquid interphase.

2.5 Evaluation

After presenting the most prominent measurement methods for surface tension and analysing applicability for high-pressure surroundings, only a few candidates stand out: Wilhelmy plate, Du Noüy ring and pendant drop. Comparing these methods with the others, the first advantage is their simplicity. This is a great advantage when thinking about the integration into high-pressure chambers. Ideally, measurements can be conducted without optical sensors, since high-pressures of more than 100 MPa require robust systems and transparency of all test liquids at high pressures cannot be ensured. Additionally, high precision force detection of less than 1 mN and reproducibility is required and a change in set up during the measurements should be avoided (e.g. changing the capillary due to changing surface tension). With the Du Noüy ring-method, all requirements for high-pressure applicability are fulfilled. With the assessment, this method is selected for further design recommendations regarding the applicability to high-pressure environments.

3 Measurements

The following measurements were done using the Du Noüy ring method at ambient conditions of 0.1 MPa and 295.15 K. Every measurement was conducted three times. All deviations within each measurement routine were below 2.3% from each other, causing the error bars to be within the dimensions of the marker itself. A calibration measurement was done using neat water with a surface tension around 72.5 mN/m. Compared to literature values in /9/, where the values of surface tension are in the range of 72.44 mN/m, the deviation is in the order of 0.1%.

The nonlinear behaviour of binary mixtures can be seen in Figure 8. Here, the surface tension is plotted over the amount of substance of ethanol. Measured values and data from literature show fairly good agreement, see /9/.

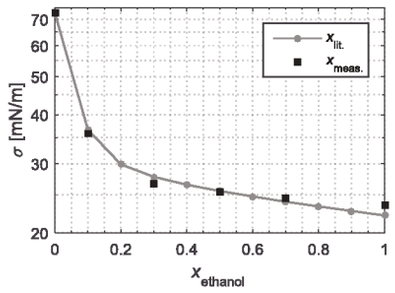

Figure 8: Comparison of literature- with measurement-data of a water-ethanol mixture after /9/.

3.1 Liquid-gas Measurements

During the injection process, a low surface tension is advantageous for a homogeneous spray distribution in the combustion chamber. The fuel is injected into air. Therefore, surface tension measurements were conducted using a fuel/air interphase. Figure 9 shows the results for common fuels after /16, 17, 18/ (left) and biofuel candidates (right). Since the commercially available fuels are mixtures and blended with additives that can vary depending on the location, the measurement results do only yield a tendency.

ROZ 95 (Super) and E10 fuel display an advantageous low surface tension between 20 and 22 mN/m, while EN 590 (Diesel) lies around 30 mN/m. These values indicate a better combustion performance for Otto-fuels in comparison with EN 590. Looking at the emissions, surface tension might be a factor for the higher soot emissions with EN 590. The range of promising fuel candidates regarding surface tension for neat components is smaller. Here, 2-Methyltetrahydrofuran, 2-MTHF, has a value of around 27 mN/m, while Di-n-Butylether, DnBE, displays a value of around 25 mN/m. The highest value can be found for 1-Octanol with 29.3 mN/m. Using a blend of 50 volume-percent 1-Octanol with DnBE and 2-MTHF respectively, the values are well within the neat fuel numbers. Almost linear behaviour can be observed using neat biofuels and blends.

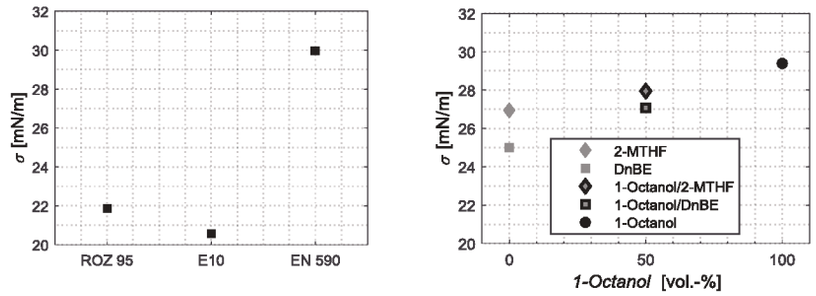

Figure 9: Surface tension values for standard fuels (left) and biofuel candidates and blends (right).

3.2 Liquid-liquid measurements

For cavitation, the interfacial tension between water and hydraulic oil can play an important role. Therefore, measurements were conducted for three hydraulic oils of differing viscosity: HLP46, HLP22 and HLP15. All HLP oils are mineral based with additives to enhance ageing-resistance, prevent corrosion and raise high-pressure usability, see /19/. Figure 10 shows the results. All oils do show surface tension values around 32.5 mN/m with an air atmosphere. If water is added and the interfacial tension between water and oil is investigated, the results vary drastically compared to the oil/air measurements. Starting from just below 20 mN/m for HLP46 and water, interfacial tension decreases with the oil viscosity. This yields 14 mN/m for HLP22 and water down to 7 mN/m for HLP15 and water. This interesting tendency can play a major role for choosing the right hydraulic oil. Nonetheless, the influence of additives within the oils which potentially react with water can also cause the behaviour seen in Figure 10. Due to a limited knowledge of the additives and their volume fraction within each respective oil, a general statement cannot be made.

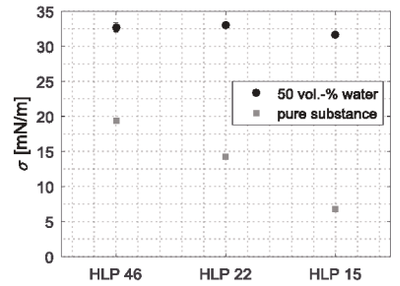

Figure 10: Influence of water on the surface tension between water and different hydraulic oils.

4 Derivation of an operational principle for high pressure tensiometers

4.1 Requirements

The presented literature survey and the investigation of the benefits and weaknesses of the different measurement approaches have shown, that the aspired measurement of surface tension under high pressure should be preferably realised by the Du Noüy ring method. Furthermore, measured surface tension of diverse fuels and biofuel candidates in figures 8 and 9 indicate a required measurement range in the order of 1-100 mN/m. Herein, a minimum resolution of 1% should be achieved. For the targeted high pressure tensiometer (IFAS HPT), the complete measurement device will probably be arranged in the high-pressure chamber of the

high pressure viscometer at IFAS, see /20/, leading to additional requirements due to confined space. Table 1 shows a comparison of different state of the art devices for ambient pressure and the resulting design parameters for the IFAS HPT to be developed.

Manufacturer and Device	**Lauda TD3 /21/**	**IMETER V6 /22/**	**Krüss K100 /23/**	**IFAS HPT**
Footprint	250 x 120 mm²	270 x 400 mm²	300 x 390 mm²	Ø 40 mm
Height	250 mm	560 mm	585 mm	200 mm
Stroke	80 mm	135 mm	110 mm	50 mm
Pressure range	Ambient pressure			up to 750 MPa
Surface tension measurement with Du Noüy ring method				
Min. surface tension	0.75 mN/m	0.5 mN/m	1 mN/m	1 mN/m
Max. surface tension	300 mN/m	1000 mN/m	2000 mN/m	100 mN/m
Resolution	0.01 mN/m	0.01 mN/m	0.001 mN/m	0.01 mN/m
Precision weighting				
Max. force	5 g / 50 mN	220 g / 2.2 N	210 g / 2.1 N	Not feasible
Resolution	0.1 mg / 1 µN	0.01 mg / 0.1 µN	0.01 mg / 0.1 µN	
Liquid density measurement				
Measurement body	External			Internal
Max. density	2000 kg/m³	1600 kg/m³	2200 kg/m³	1500 kg/m³
Resolution	1 kg/m³	1 g/m³	1 kg/m³	0.1 kg/m³

Table 1: Comparison of different state of the art devices /21, 22, 23/ and IFAS HPT under development.

Thereof, the required resolution of the force sensing device can be deduced. The simplified correlation of surface tension σ and force F_{ST} on the Du Noüy ring in equation (13) enables the definition of the required forces /24/.

$$\sigma = \frac{F_{ST}}{4\pi \cdot r} \tag{13}$$

Employing a Du Noüy ring according to DIN EN 14370 with a radius r of 9.75 mm results in tension forces of 0.123 mN to 12.25 mN in the aspired surface tension regime. The weight of the Du Noüy ring and the movable part of the force detecting device adds to the tension force, leading to a significant offset. Thus, huge demands on the precision of the force sensing device result whether the smallest values for surface tension have to be measured with reasonable accuracy.

To allow for precise measurements, commercially available devices possess electromagnetically compensated weigh cells. Therein, a voice coil actuator (VCA) holds the load in constant position, which is fed-back by a contactless position sensor. As the VCA possesses a completely linear force/current characteristics in fixed position the load is proportional to the measured current through the VCA's coil. Recalibration is achieved by one or more integrated calibration weights in the weigh cell assembly, so that changes in current/force gain can be automatically corrected /25/. Unfortunately, such devices do not fit in the high pressure chamber of the high pressure test rig and the change in density of the surrounding medium over pressure interacts with the measurement and calibration devices and thus leads to strong deviations of the measured values and calibration.

Hence, the key challenge in designing a high pressure tensiometer for liquid/liquid and liquid/gas applications lies on the one side in the confined space and required measurement accuracy and on the other side in the ability of remote recalibration under high pressure. The last challenge will be discussed in the following subchapter.

4.2 Recalibration strategy

Supposing an ideal sensor which possesses a completely linear force current relationship with force gain k, the effect of changing density on measurement results still prohibits an exact determination of the surface tension. Taking into account a volume of the moving measurement device V_M with a mean density ρ_M, and the density of the surrounding fluid ρ_{fl}, the measured force yields

$$F = k \cdot i = V_M \cdot g \cdot (\rho_M - \rho_{fl}) + F_{ST} \tag{14}$$

Supposing a volume V_M of 5 cm³, a small inaccuracy in density ρ_{fl} or ρ_M of 1 kg/m³ already leads to a deviation in measured force signal of 49.05 µN, which equals a change in surface tension of 0.4 mN/m. Hence, to achieve sufficient measurement accuracy over a wide pressure and temperature span, a continuous in situ recalibration of the fluid density ρ_{fl} by the tensiometer is required.

As the accuracy of the measurement device is also highly affecting measurement accuracy, the force gain of the measurement device should also be recalibrated under operating conditions. Recalibration of sensor and fluid density can be achieved by use of two incompressible calibration weights (volumes V_1 and V_2) of different densities ρ_1 and ρ_2 inside the tensiometer. Assuming, that the second calibration weight can only be added to the system if the first one is applied and calibration is achieved without surface tension acting on the Du Noüy ring, the equations describing the system with (index "1" and "12") and without (index "0") calibrations weights are:

$$F_0 = k \cdot i_0 = g \cdot V_M \cdot (\rho_M - \rho_{fl}) \tag{15}$$

$$F_1 = k \cdot i_1 = g \cdot \left(V_M \cdot (\rho_M - \rho_{fl}) + V_1 \cdot (\rho_1 - \rho_{fl})\right) \tag{16}$$

$$F_{12} = k \cdot i_{12} = g \cdot \left(V_M \cdot (\rho_M - \rho_{fl}) + V_1 \cdot (\rho_1 - \rho_{fl}) + V_2 \cdot (\rho_2 - \rho_{fl})\right) \tag{17}$$

As a result, the force gain of the sensor k and the fluid density ρ_F can be determined as:

$$k = \frac{g \cdot V_2 \cdot (\rho_1 - \rho_2)}{(i_1 - i_0) \cdot \frac{V_2}{V_1} - (i_{12} - i_1)} \tag{18}$$

$$\rho_{fl} = \frac{V_1 \cdot \rho_1 \cdot (i_{12} - i_1) - V_2 \cdot \rho_2 \cdot (i_1 - i_0)}{V_1 \cdot (i_{12} - i_1) - V_2 \cdot (i_1 - i_0)} \tag{19}$$

Thus, online recalibration of the sensing device and the surrounding density is feasible. Nevertheless, a technology to implement a highly linear and stroke independent sensor, the actuator to move the Du Noüy ring and the actuators to apply two calibration weights in the confined cylindrical space still pose a challenge, which has to be met in the future. A promising way could be the integration of a VCA as sensing and driving element and two electromagnetic actuators holding the at least partially ferromagnetic weights. There for, subsequent studies on linearity of suitable VCA's and on a frictionless linear bearing for its coil are necessary. Also, a stroke sensor or at least velocity estimation using the VCA's voltage has to be considered for surface tension measurement.

5 Summary and Conclusion

The paper illustrates the necessity of high-pressure surface tension measurements. With a first concept, some challenges are addressed. In order to investigate the applicability of the proposed method, a first prototype needs to be developed.

In this paper, the importance of surface tension measurements was shown to support design processes as well as the understanding of fluid flow phenomena. First, an introduction was given with examples regarding injector-technology, chemical reactors and hydraulics. With the introduction to pressure dependent surface tension, common measurement methods were introduced and evaluated concerning the applicability in high-pressure environments. As a result, the Du Noüy ring method was identified as a suitable candidate for the adaption to high-pressure. Afterwards, measurements results for ambient conditions were presented for different fuel and biofuel candidates as well as different hydraulic oils. Moreover, the tendency for a lower interfacial tension between water and oil for lower viscosity oils was shown. Afterwards, an analysis of current commercial Du Noüy ring tensiometers was performed and requirements for a high-pressure application were derived. With these requirements a first concept was presented.

6 Acknowledgements

This work was performed as part of the Cluster of Excellence "Tailor-Made Fuels from Biomass", which is funded by the Excellence Initiative by the German federal and state governments to promote science and research at German universities.

Nomenclature

Variable	*Description*	*Unit*
d	Diameter	[m]
F	Force	[N]
f	Correction factor	[-]
g	Gravitation	[m/s²]
H	Shape dependent parameter	[-]
h	Height	[m]
i	Current	[A]
k	Calibration factor	[N/A]
L	Length	[m]
Oh	Ohnesorge number	[-]
p	Pressure	[Pa]
R	Radius	[m]
r	radius	[m]
Re	Reynolds number	[-]
t	Thickness	[m]
V	Volume	[m³]
v	Speed	[m/s]
w	Weight fraction	[-]
η	Dynamic viscosity	[Pa s]
ρ	Density	[kg/m³]
σ	Surface Tension	[N/m]
φ	Meniscus angle	[°]
ω	Rotational velocity	[1/s]

Index	*Description*
0	Initial
1	Calibration weight 1
2	Calibration weight 2
12	Calibration weights 1 and 2 together
bubble	Properties of a bubble
e	Equatorial
fl	Fluid
M	Moving measurement device
s	Additional
ST	Acting on Du Noüy ring

Abbreviation	*Description*
$2-MTHF$	2-Methyltetrahydrofuran
$E10$	Unleaded fuel with 5-10 vol.% ethanol
$EN\ 590$	Diesel fuel
$dgde$	Diethylene glycol diethyl ether
$DnBE$	Di-n-Butylether
$E10$	Gasoline with 10% ethanol
HLP	Minreal based hydraulic oil with corrosion and high-pressure additives
HPT	High-pressure tensiometer
$IFAS$	Institute for fluid power drives and controls
$ROZ\ 95$	Unleaded fuel (Super)
VCA	Voice coil actuator

References

/1/ Ohnesorge, W., *Formation of drops by nozzles and the breakup of liquid jets* – Journal of Applied Mathematics and Mechanics 16, p. 355-358, 1936

/2/ Li, D., *Encyclopedia of Microfluidics and Nanofluidics* – Springer, New York, United States, 2015

/3/ Schneider, B.M., *Experimentelle Untersuchungen zur Spraystruktur in transienten, verdampfenden u nicht verdampfenden Brennstoffstrahlen unter Hochdruck* – Dissertation, ETH Zürich, 2003

/4/ Kreutzer, M.T. et al., *Multiphase monolith reactors: Chemical reaction engineering of segmented flo microchannels* – Chemical Engineering Science 60, p. 5895-5916, 2005

/5/ Longhitano, M., Murrenhoff, *H., EXPERIMENTAL INVESTIGATION OF AIR BUBBLE BEHAVIOU IN STAGNANT MINERAL OILS* – Proceedings of the ASME/BATH 2015 Symposium on Fluid Powe Motion Control, Chicago, Illinois, USA, 2015

/6/ Krahl, D., et al., *Visualization of cavitation and investigation of cavitation erosion in a valve* - Proceedings of the 10th International Fluid Power Conference, Dresden, Germany, 2016

/7/ Murrenhoff, H., *Fundamentals of Fluid power – Part 1: Hydraulics* - 8th Edition, Shaker, Aachen, 20

/8/ Nielsen, C.J., *Density and Surface Tension of Aqueous H2SO4 at Low Temperature* – Journal of Chemical Engineering Data 43, p. 617-622, 1998

/9/ Wohlfarth, C., Surface Tension of Pure Liquids and Binary Liquid Mixtures – Group IV: Physical Chemistry Volume 24, Supplement to IV/16, Springer, Berlin, Germany, 2008

/10/ Dechoz, J., Roze, D., *Surface tension measurement of fuels and alkanes at high pressure under differe atmospheres* - Applied Surface Science 229, p. 175-182, 2004

/11/ Sachs, W., Meyn, V., *Pressure and temperature dependence of the surface tension in the system natu gas/water* – Colloids and Surfaces A: Physicochemical and Engineering Aspects 94, p. 291-301, 199

/12/ Drelich, J., et al., *MEASUREMENT OF INTERFACIAL TENSION IN FLUID-FLUID SYSTEMS* – Encyclopedia of Surface and Colloid Science, Marcel Dekker Inc., New York, 2002

/13/ Misak, M.D., *Equations for determining 1/H versus S values in computer calculations of interfacial tension by pendent drop method* – J. Colloid Interface Science 27, p. 141-142, 1968

/14/ *Manual of the Spinning Drop Tensiometer Site 04*, Krüss GmbH, Hamburg, Germany, 1995

/15/ Harkins, W.D., Brown, F.E., *The determination of surface tension (free surface energy), and the weig of falling drops: the surface tension of water and benzene by the capillary height method*, J. Am. Che Soc. 41, p. 499-525, 1919.

/16 N, N., *DIN EN 228 - Automotive fuels - Unleaded petrol - Requirements and test methods* – Beuth, Berlin, Germany, 2017

/17 N, N., *DIRECTIVE 2009/28/EC OF THE EUROPEAN PARLIAMENT AND OF THE COUNCIL of 2. April 2009 on the promotion of the use of energy from renewable sources* – Brussels, Belgium, 2009

/18 N, N., *EN 590 – Automotive fuels - Diesel - Requirements and test methods* – Brussels, Belgium, 201

/19/ N, N., *DIN 51524-2 - Druckflüssigkeiten – Hydrauliköle – Teil2: Hydrauliköle HLP, Mindestanforderungen* – Deutsches Institut für Normung e. V., Berlin, Deutschland, 2017

/20/ Drumm, S.M., *Entwicklung von Messmethoden hydraulischer Kraftstoffeigenschaften unter Hochdru* Dissertation, RWTH Aachen University, Shaker, Aachen, 2012.

/21/ N, N., *Operating Instructions - TD3*, LAUDA DR. R. WOBSER GmbH & Co. KG, 2009.

/22/ N, N., *IMETER V6*, http://www.imeter.de, visited on November 10, 2017.

/23/ N, N., *FORCE TENSIOMETER – K100 – SPECIFICATIONS*, KRÜSS, 2018.

/24/ N, N., *DIN EN 14370 - Grenzflächenaktive Stoffe – Bestimmung der Oberflächenspannung*, Beuth, Berlin, Germany, 2004.

/25/ Burkhard, H.-R., Schneider, F., *EP 2533024 A1 - Force transferring device with attachable calibratic weight*, Patent, 2011